Aeroacoustic Prediction and Measurements of Jet-Airfoil Interaction Noise

J. Christophe[1], C. Schram[2], M. Tournour[3]

[1] *von Karman Institute for Fluid Dynamics, Belgium, Email: christju@vki.ac.be*

[2] *LMS International, Belgium, Email: christophe.schram@lmsintl.com*

[3] *LMS International, Belgium, Email: michel.tournour@lmsintl.com*

Introduction

Aerodynamic noise is a serious concern in a number of applications where turbulence interacts with rotating blades. CPU cooling fans, for example, are nowadays considerably louder than before due to the constant growth of the processor performance and resulting heat release. In automotive and locomotive applications as well, the noise levels that can be emitted by the engine cooling fans are very strictly limited, either because of the economic competition or because of the legislator. Modern aeroacoustic prediction tools have been developed and commercialized thereto, which are often based on the application of the Lighthill's analogy [1] and the interpretation of unsteady flow field data as equivalent acoustical sources. In the modern implementation of this analogy, the transient features of the flow field are modeled by more or less expensive Computational Fluid Dynamics (CFD) approaches. Unsteady Reynolds-Averaged Navier-Stokes (RANS), Large Eddy Simulation (LES), Detached Eddy Simulation (DES) or Scale Adaptative Simulation (SAS) are being increasingly used for realistic industrial configurations, with varying degrees of success depending in good part on the numerical cost due to the mesh size, scheme accuracy, etc. The present work is aimed at reaching the best possible compromise between accuracy and cost, by combining several approaches described below.

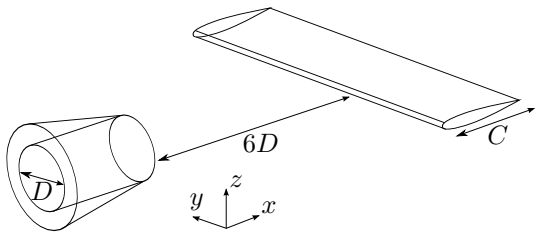

Figure 1: Configuration geometry.

This work considers the noise produced by the turbulent region of a jet interacting with a NACA 0012 airfoil placed at zero angle of attack, its leading edge located at 6 jet diameters D from the nozzle outlet (Figure 1). Compared to other leading edge noise applications, like the interaction of a rod-cylinder with an airfoil [2] where dominant frequencies appear in the sound predictions depending on the shedding frequency of the cylinder, this application proposes a broadband spectrum, the airfoil being placed in the transitional region of the jet. Furthermore, the interacting flow being non-uniform in the spanwise direction, this application reproduces conditions similar to a rotating machine, like fans, for which upstream conditions are non-uniform along the blade, in term of velocity speed, turbulence intensity and coherence length scale. This jet-airfoil interaction case is then a interesting starting point for development of new methods dedicated to rotating machines.

Flow configuration

The nozzle outlet diameter is equal to $D = 0.041$ m. The chord length C of the airfoil is equal to D, and the section is constant over the span which extends spanwise up to the quiescent flow region in order to avoid tip noise. The outlet velocity magnitude U_0 is fixed to 13.2 m/s resulting in a Reynolds number based on the chord length $Re = U_0 C/\nu = 36,000$, and a Mach number $Ma = U_0/c_0 = 0.04$, where c_0 is the speed of sound. The boundary layer developed at the outlet of the nozzle, downstream of the contraction, shows a laminar Blasius profile for a range of velocities from 5 to 40 m/s.

Experimental setup

The jet discharges in an anechoic room, with dimensions $4 \times 3 \times 4$ m^3, and cut-off frequency of 350 Hz. Velocity measurements have been obtained by hot wire anemometry. Series of 2^{16} points were acquired with a sampling frequency of 35 kHz. Experimental velocity data are available for four profiles in the radial direction ($2D$, $4D$, $5D$ and $8D$) and one profile along the axial direction. Sound measurements are taken with Bruel & Kjaer microphones. A high-pass filter of 100 Hz and a low-pass filter of 12 kHz are used. The sampling frequency is 2^{15} Hz and measurements are taken during 1 s. These measurements are available at a point distance of 0.3 m from the airfoil, in its median plane and perpendicularly to the jet axis.

Numerical setup

Flow modeling

An incompressible flow computation is considered, given the low Mach number. Based on the characteristic dimension of the airfoil and on the jet outlet velocity, a non-dimensional simulation time $t' = tU_0/C$ is defined, where t is the physical time of the computation.

The unsteady flow around the airfoil is computed with the Large Eddy Simulation (LES) solver of the commercial software Fluent Rev 6.3. The computational domain

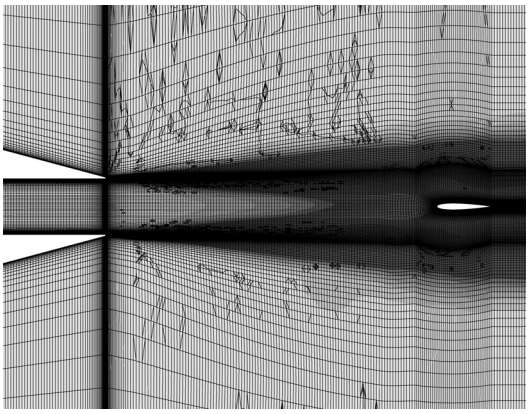

Figure 2: Mesh cells repartition in the $x-z$ plane.

extends to $5D$ in the radial direction and to $16D$ in the axial direction, including a $2D$ long nozzle before the jet outlet and a $5D$ long sponge zone at the end of the domain to prevent any significant reflections. The $2D$ long nozzle is introduced in order to have more physical and structured perturbations at the jet outlet. The flow is resolved on a mesh of 2.8 million hexahedral cells and refined near the solid boundaries, around the jet and around the wing in order to reach $y^+ < 2$ in these regions (Figure 2).

The dynamic Smagorinsky type eddy viscosity is used as subgrid-scale model and second order discretization schemes are used both in space and time. A time step $\Delta t = 10^{-5}$ s is used, yielding a CFL number below 0.6. Zero pressure condition is set at the boundaries of the domain. A sponge zone is placed at the end of the computational domain in order to avoid numerical pressure disturbances due to the vortices crossing the downstream boundary [3].

Unsteady statistics (mean and RMS values) and source data have been collected during a non-dimensional acquisition time of $t' = 70$.

Acoustic methods

Two different approaches are combined for the prediction of the aerodynamic sound, to cover the lowest and highest ranges of frequencies respectively. The low frequency range corresponds to the frequencies that are effectively resolved by the LES flow model on the present mesh. The sources distributed on the airfoil are acoustically compact for these frequencies (up to about 1 kHz), and the Lighthill/Curle analogy is employed therefore. For the highest frequencies, the LES model applied to the present mesh proves unable to capture the relevant turbulent scales of the jet, but these scales are assumed to exhibit a certain degree of local isotropy and homogeneity such that a statistical model, based on Amiet's theory, is used. The two questions we want to address are *i*) whether the two approaches give acceptable results in their respective asymptotic frequency ranges of application, and *ii*) whether they match in a mid-frequency range, in which case they could be combined to cover the full noise spectrum.

Curle's analogy

Curle [4] provides the following integral solution of Lighthill's analogy [1], in the presence of solid surfaces in the source region:

$$\rho'(\mathbf{x},t) = \frac{\partial^2}{\partial x_i \partial x_j} \iiint_V \left[\frac{T_{ij}}{4\pi c_0^2 |\mathbf{x}-\mathbf{y}|}\right] \mathrm{d}^3\mathbf{y} - \frac{\partial}{\partial x_i} \iint_{\partial V} \left[\frac{p' n_i}{4\pi c_0^2 |\mathbf{x}-\mathbf{y}|}\right] \mathrm{d}^2\mathbf{y} \quad (1)$$

where ρ' is the acoustic density perturbation, $T_{ij} = \rho v_i v_j + (p' - c_0^2 \rho')\,\delta_{ij} - \sigma_{ij}$ is the Lighthill's tensor where p is the pressure, v_i is the i-th velocity component and σ_{ij} is the viscous stress tensor, and where the free-field Green's function has been used. In the surface integral of (1), the viscous contribution of T_{ij} has been neglected, the surface is assumed non-vibrating and with no-slip, and the bracketed terms are to be evaluated at the retarded time $t^* = t - |\mathbf{x}-\mathbf{y}|/c_0$.

Curle [4] demonstrated that for a compact distribution of sources at low Mach numbers, the contribution from the volume integral in (1) is of quadrupolar character and can be neglected. We proceed accordingly in this work by retaining the dipolar source only. The acoustic results presented below for Curle's analogy have been obtained using a boundary integral implementation of this analogy in the commercial Boundary Element solver Virtual.Lab Acoustics Rev 8B [5].

Amiet's theory - Leading edge formulation

We use Amiet's theory for incoming turbulence noise [6] and its extension by Moreau *et al.* [7] to predict the high-frequency part of the airfoil-jet interaction noise spectrum. Incoming flow non-homogeneities, described as a superposition of spatial Fourier modes (gusts), are assumed to be convected in a frozen way over the airfoil. The aerodynamic response of the airfoil is obtained by a linearized theory assuming a small thickness, camber and angle of attack. The non-compactness effects, in the chordwise direction, are accounted for in the analytical calculation of an aeroacoustic transfer function.

An incoming gust is represented in terms of its longitudinal and transversal wavenumber components, k_x and k_y. The far-field acoustic PSD is, at the listener position $\mathbf{x}$:

$$S_{PP}(\mathbf{x},\omega) = \left(\frac{\omega z \rho_0 b}{c_0 \sigma^2}\right)^2 U\pi d \int_{-\infty}^{\infty} \frac{\sin^2[d\,(k_y+K_y)]}{\pi d\,(k_y+K_y)^2} \left|\mathcal{L}(\mathbf{x},k_x,k_y)\right|^2 \Phi_{ww}(k_x,k_y)\,\mathrm{d}k_y, \quad (2)$$

where b and d are respectively the half-chord and half-span, U is the gust incoming velocity, $k_x = \omega/U$ and $K_y = \omega y/c_0\sigma$, $\sigma^2 = x^2 + \beta^2(y^2+x^2)$, $\beta^2 = 1-M^2$, M is the Mach number and Φ_{ww} is the turbulent energy spectrum for the wall-normal gust velocity component. The aeroacoustic tranfert function $\mathcal{L}$ combines the unsteady aerodynamic response of the airfoil to an incident gust and the corresponding acoustic propagation including leading and trailing edge scattering effects.

Amiet's theory for spanwise-varying flow conditions

The main restrictions of the theory depicted above concern the assumed uniform upstream flow conditions along the airfoil span. In several industrial applications, as in wind turbines, fans, helicopter rotors or airfoil in jets [8], the properties of the flow (velocity, turbulence intensity, integral length scale of turbulence) are not constant along the span, which does not allow using such theories. Rozenberg [9] attempted to treat spanwise-varying conditions in case of trailing edge noise by dividing the complete airfoil in strips, having each their own flow conditions. The overall noise radiated being the summation of the noise emitted by each one of the airfoil strips, assuming a decorrelation between the strips. This strip method has been further extended and validated by Christophe [10], and the latter improvements are used in the present work.

Aerodynamic results

Figure 3 shows a snapshot of the instantaneous flow field computed around the airfoil. The coherent structures are visualized with the second invariant of the velocity gradient tensor.

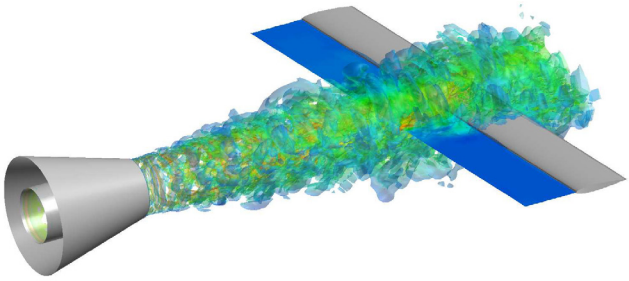

Figure 3: Instantaneous flow field around the airfoil, and spatial correlation extraction plane.

Statistics of the time averaged velocity and of the turbulent intensity based on the x and z velocity components are extracted from the unsteady LES computation and compared with experimental results in the same conditions (Figure 4) along the x-axis. For all cases, numerical and experimental profiles of the axial mean velocity are in rather good agreement along all the axial direction. The agreement is less good for the turbulence intensity, in the range $0 < x/D < 4$, but the simulated turbulence intensity matches fairly the experiments at the interaction point $x/D = 6$.

Figure 5 illustrates the velocity magnitude power spectral density for a point placed on the axis of the jet at $x/D = 5$. The comparison with the experimental results shows that the low frequency range of the power spectrum is well reproduced by the CFD computations up to about 1 kHz.

Acoustic results

Amiet's method is based on an assumption on the shape of the turbulent energy spectrum approaching the airfoil.

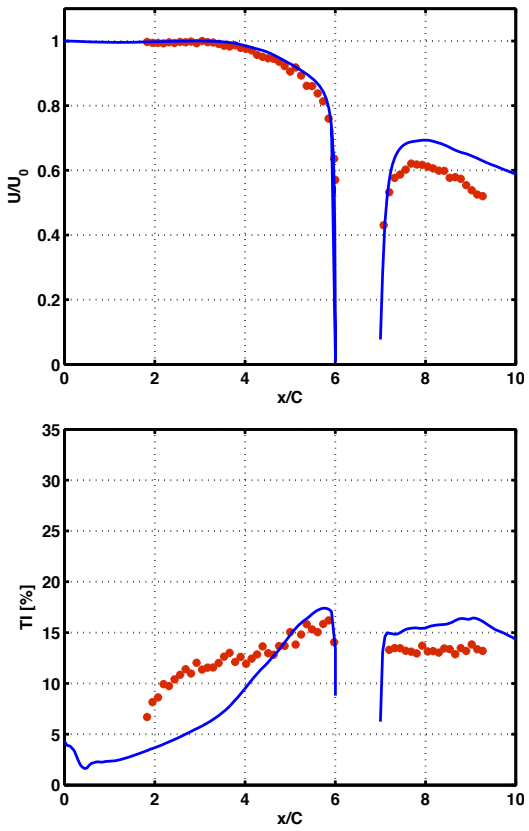

Figure 4: Comparison of experimental measurements with numerical computations : mean velocity profiles (up) and turbulence intensity profiles (bottom) along the x-axis.

In the present study, the von Kármán model is considered for the two-dimensional wavenumber turbulent energy spectrum Φ_{ww}:

$$\Phi_{ww}(k_x, k_y) = \frac{4}{9\pi} \frac{\overline{u^2}}{k_e^2} \frac{\hat{k}_x^2 + \hat{k}_y^2}{(1 + \hat{k}_x^2 + \hat{k}_y^2)^{7/3}}, \qquad (3)$$

where $\hat{k}_i$ are the wavenumbers made non-dimensional by $k_e = (\sqrt{\pi}/\Lambda)\,\Gamma(5/6)/\Gamma(1/3)$. The two relevant parameters of this model are the RMS of the squared velocity $\overline{u^2}$, directly related to the turbulence intensity, and the turbulence length scale Λ. The length scale is here determined by integrating the two-dimensional spatial auto-correlation of the upwash velocity component, extracted from a plane illustrated in blue in Figure 3. Details on the procedure are given by Christophe [10].

Spanwise-varying values for the incoming velocity, turbulence intensity and correlation length are used for the normalisation of the von Kármán spectrum and its application in Amiet's Equation 2. It was observed that 20 segments over the span of $3C$ are enough to discretize the spanwise varying conditions correctly and to ensure converged sound predictions. The receiver position is placed at $(x, y, z) = (0, 0, 7.3C)$. A comparison between the Sound Pressure Level predicted using Amiet's theory and sound measurements is shown in Figure 6. The maximum deviation between the prediction based on Amiet's theory and the experimental results is about 5 dB in the range 500-10000 Hz. Larger deviations are

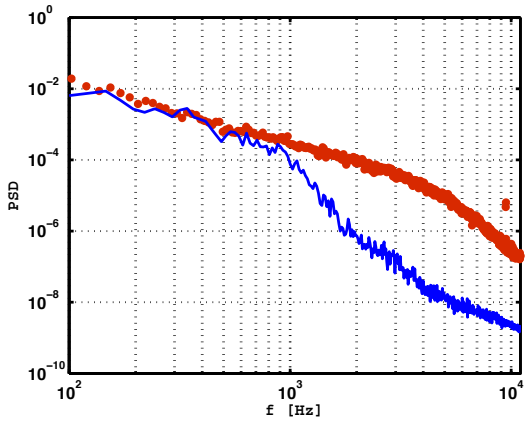

Figure 5: Comparison of experimental measurements with numerical computations : Power Spectrum Density of velocity magnitude fluctuations at $(x, y) = (5D, 0)$ (bottom).

observed at the lowest frequencies, corresponding to the large anisotropic scales of the turbulence for which the von Kármán spectrum is not suited. In contrast, the deterministic method is seen to provide reasonable sound prediction for the low frequencies, i.e. up to 1000 Hz for the present CFD mesh size and numerical schemes.

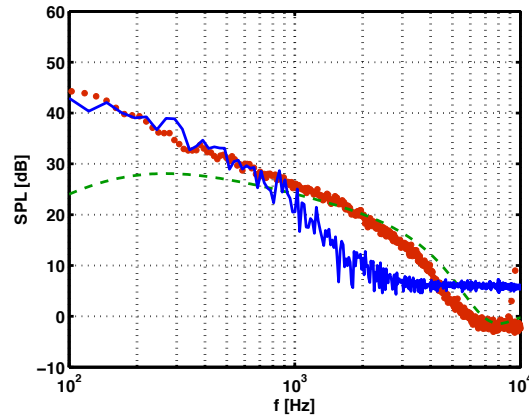

Figure 6: Comparison of sound measurements with numerical predictions using Curle's analogy and Amiet's theory.

Conclusions

Curle's analogy permits a straightforward numerical procedure for the prediction of turbulence-body interaction broadband noise, especially at low Mach numbers when the quadrupolar contribution can be neglected with respect to the dipolar one. However, by comparing simulated and measured turbulence velocity spectra, it is shown that the effective cut-off frequency that can be reached by incompressible Large Eddy Simulation with an affordable mesh size does hardly exceed 1 kHz in the present case, while a sound prediction up to a few kHz is usually desired by acoustic engineers. We propose therefore to combine a deterministic sound prediction method based on transient CFD for the low frequency range, with a procedure based on Amiet's theory that models the statistical properties of turbulence for the highest frequencies. The resolved part of turbulence is used to tune the statistical model taking into account spanwise variations of the incoming turbulence, which is of importance when dealing with rotating machineries for example. The results demonstrate that each approach yields a fair agreement with the experimental data within its range of applicability. Furthermore, the deterministic and statistic approaches show a satisfactory overlap in the mid-frequency range. This suggests the possibility to combine both methods to cover the full frequency range.

Acknowledgements

This work was supported by a fellowship from the Belgian regional *Fonds pour la Formation à la Recherche dans l'Industrie et dans l'Agriculture* (FRIA).

References

[1] M. J. Lighthill. On sound generated aerodynamically. Part I. General theory. Proceeding of the Royal Society of London **A211** (1952), 564-587.

[2] D. Casalino, M. C. Jacob, and M. Roger. Prediction of rod-airfoil interaction noise using the Ffowcs Williams and Hawkings analogy. AIAA Journal **41** (2003), 182-191.

[3] T. Colonius, S. K. Lele, and P. Moin. Boundary conditions for direct computation of aerodynamic sound generation. AIAA Journal **31**(9) (1993), 1574-1582.

[4] N. Curle. The influence of solid boundaries upon aerodynamic sound. Proceeding of the Royal Society of London, **A231** (1955), 505-514.

[5] LMS International. Virtual.Lab 8B User's Manual (2008), Leuven.

[6] R. K. Amiet. Acoustic radiation from an airfoil in a turbulent stream. Journal of Sound and Vibration **41**(4) (1975), 407-420.

[7] S. Moreau, M. Roger, and V. Jurdic. Effect of angle of attack and airfoil shape on turbulence-interaction noise. 11th AIAA/CEAS Aeroacoustics Conference and Exhibit (2005), AIAA Paper 2005-2973, Monterey, May 23-25.

[8] J. Christophe, J. Anthoine, P. Rambaud, C. Schram, F. Mathey, and S. Moreau. Prediction of incoming turbulent noise using a combined numerical/semi-empirical method and experimental validation. 13th AIAA/CEAS Aeroacoustics Conference (2007), AIAA Paper 2007-3468, Rome, May 21-23.

[9] Y. Rozenberg, M. Roger, A. Guédel, and S. Moreau. Rotating blade self noise : Experimental validation of analytical models. 13th AIAA/CEAS Aeroacoustics Conference (2007), AIAA Paper 2007-3709, Rome, May 21-23.

[10] J. Christophe. Airfoil noise: Hybrid approaches. Aerodynamic Noise from Wall-Bounded Flows (2009). von Karman Institute Lecture Series, Rhode-St-Genèse.